The Aharonov–Bohm effect in a side-gated graphene ring

New Journal of Physics
The open-access journal for physics

The Aharonov–Bohm effect in a side-gated graphene ring

Magdalena Huefner[1,2], Françoise Molitor[2], Arnhild Jacobsen, Alessandro Pioda, Christoph Stampfer[3], Klaus Ensslin and Thomas Ihn

Solid State Physics Laboratory, ETH Zurich, Switzerland
E-mail: huefner@phys.ethz.ch

New Journal of Physics **12** (2010) 043054 (10pp)
Received 24 November 2009
Published 30 April 2010
Online at http://www.njp.org/
doi:10.1088/1367-2630/12/4/043054

Abstract. We investigate the magnetoresistance of a side-gated ring structure etched out of single-layer graphene. We observe Aharonov–Bohm oscillations with about 5% visibility. We are able to change the relative phases of the wave functions in the interfering paths and induce phase jumps of π in the Aharonov–Bohm oscillations by changing the voltage applied to the side gate or the back gate. The observed data can be interpreted within existing models for 'dirty metals'.

Contents

[1] Author to whom any correspondence should be addressed.
[2] Both authors have contributed equally to this work.
[3] Current address: JARA-FIT and II Institute of Physics, RWTH Aachen, Germany.

1. Introduction

Less than a decade ago, single-layer graphene sheets were isolated for the first time [1]. Since then, amazing progress in the fabrication of increasingly more complex nanostructures has been made. While the earlier research interests were focused on the most basic nanostructures, e.g. graphene constrictions or nanoribbons [2]–[7], soon different groups were able to form increasingly complex structures such as quantum dots [8]–[11] and double dots [12]. Despite this increasing control over very complex nanostructures, only one experimental publication on graphene rings is available [13]. Predominantly, the theoretical aspects of the Aharonov–Bohm effect [14, 15] in graphene have been addressed in the literature [16, 17]. One consequence of interference (weak localization) has been studied in graphene flakes [18]–[20] with the outcome that weak localization can only be observed in the presence of intervalley scattering.

Nanoscale rings have been studied in nanostructures of a variety of different materials including carbon materials such as carbon nanotubes [21, 22]. Only recently, the Aharanov–Bohm effect has been observed for the first time in a two-terminal graphene ring structure [13]. In this experiment, the visibility of the Aharonov–Bohm oscillations was found to be less than 1% at low magnetic fields. It was speculated that this small value might be due to inhomogeneities in the two interferometer arms, leading to a tunneling constriction that suppressed the oscillations.

In this paper, we present four-terminal magnetotransport through a graphene ring of smaller size than the devices studied in [13]. We demonstrate h/e-periodic Aharonov–Bohm oscillations with a visibility that is increased by a factor of up to 10 compared to the two-terminal case [13]. In addition, our graphene ring has better tunability as it is equipped not only with a back gate, which allows us to change the charge carrier density in the complete sample, but also with side gates, allowing a local tuning of the charge carrier density in one of the arms. This added tunability allows us to demonstrate that a π-phase shift of the oscillations can be achieved by changing a gate voltage. The observed data can be interpreted within existing models for dirty metals.

2. Sample and setup

Figure 1(a) displays a scanning force micrograph of the graphene ring studied in this work. The graphene flakes are produced by mechanical exfoliation of natural graphite, and deposited on a highly doped Si wafer covered by 295 nm of silicon dioxide [1]. Thin flakes are detected by optical microscopy, and Raman spectroscopy is used to confirm the single-layer nature of the selected graphitic flakes [23, 24]. In figure 1(b), we show the Raman spectrum of the graphene flake used for the fabrication of the investigated graphene ring device (figure 1(a)). The spectrum has been recorded before structuring the flake and the narrow, single Lorentzian shape of the 2D line is proof of the single-layer nature [23, 24]. Electron beam lithography followed by reactive ion etching is used to define the structure. The contacts are added in a second electron beam lithography step, followed by the evaporation of Cr/Au (2 nm/40 nm) [9].

All the measurements presented in this work were performed in an He^3 cryostat at a base temperature of $T \approx 500$ mK. Standard low-frequency lock-in techniques are used to measure the resistance by applying a constant current. A magnetic field is applied perpendicular to the sample plane.

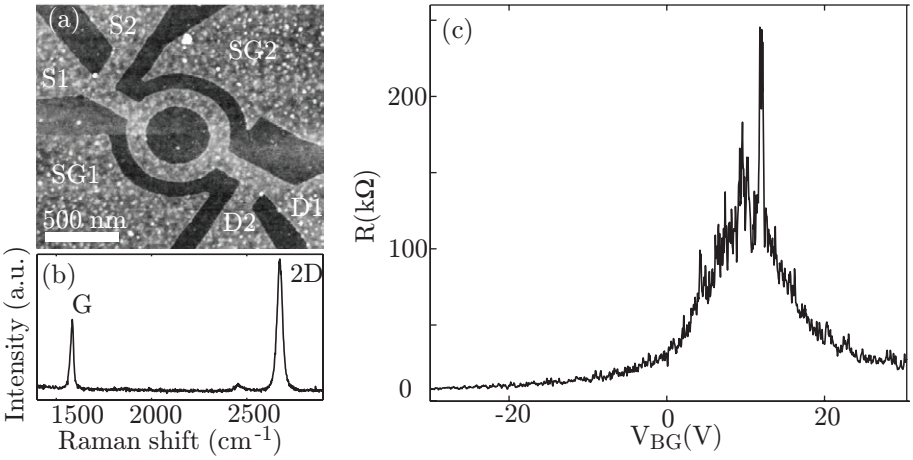

Figure 1. (a) Scanning force micrograph of the ring structure studied in this work. The ring has an inner radius of about 200 nm and an outer radius of about 350 nm. On each end of the ring structure, there are two graphene contact pads labeled S1/2 and D1/2, allowing us to perform four-terminal resistance measurements. The side gates labeled SG1 and SG2 are located 100 nm away from the structure. (b) The Raman spectrum of the same flake before processing. The spectrum was recorded using a laser excitation wavelength of 532 nm. (c) Four-terminal resistance across the ring structure as a function of back gate voltage, with both side gates grounded. The measurement is recorded at a temperature of 500 mK with a constant current of 10 nA.

3. Results and discussion

3.1. *Characterization at zero magnetic field*

Figure 1(c) displays the resistance of the ring as a function of applied back gate voltage V_{BG} measured in a four-terminal configuration. The ring itself is connected via two graphene ribbons of 150 × 350 nm size (graphene leads) to a branching that ends in larger graphene areas, where four gold contacts are used to measure the resistance. The measured resistance is composed of the ring resistance itself and the resistance of the graphene leads.

The measured resistance R_{meas} consists of the following parts: $R_{meas} = 2R_{gl} + R_{ring}$, where R_{gl} is the resistance of one graphene lead and R_{ring} is the resistance of the ring itself. In a semiclassical Drude picture, these resistances can be calculated from the geometric aspect ratios (i.e. the length L and the width W) of the graphene lead (gl) and one arm of the graphene ring (aring) as follows: $R_{meas} = (2(L_{gl}/W_{gl}) + \frac{1}{2}(L_{aring})/(W_{aring}))\frac{1}{\sigma} = 7.5\frac{1}{\sigma}$, where σ is the conductivity at a given density. Hence, the ring contributes about 38% to the measured resistance and the graphene leads about 62%.

As seen in figure 1(c), the charge neutrality point occurs at $V_{BG} \approx 10$ V. The high resistance observed at the charge neutrality point is related to the small width $W = 150$ nm of the ring arms [6]. However, this width was chosen large enough so that strong localization of charge carriers leading to Coulomb-blockade-dominated transport in narrow ribbons [6, 7] is not dominant. A rough estimate of the mobility taking into account the geometry of the structure and using the parallel plate capacitor model leads to $\mu \leqslant 5000\,\mathrm{cm^2\,Vs^{-1}}$, comparable to the

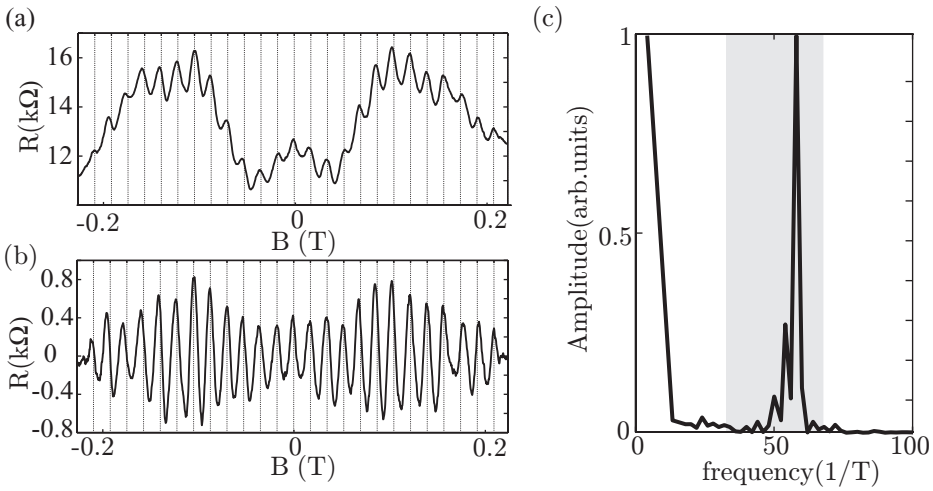

Figure 2. Four-terminal resistance across the ring as a function of magnetic field, recorded at $V_{BG} = -5.789$ V with a constant current of 5 nA. In (a), the raw data are shown. For (b) the background resistance has been subtracted as described in the text. (c) Fourier transform of the trace.

value quoted for the material used in [13]. For the typical back gate voltage $V_{BG} = -5.8$ V used for most of the measurements presented in this paper, the parallel plate capacitor model gives the sheet carrier density $p_s = 1.2 \times 10^{12}\,\mathrm{cm}^{-2}$.

We identify the relevant transport regime in terms of appropriate length scales. The Fermi wavelength corresponding to the carrier density mentioned above is $\lambda_F = \sqrt{4\pi/p_s} = 33$ nm. For comparison, at the same density, the mean free path is $l = \hbar\mu\sqrt{\pi p_s}/e \approx 65$ nm. This is less than half of the width W of the arms and much smaller than the mean ring radius $r_0 = 275$ nm and its corresponding circumference $L = 1.7\,\mu$m. Therefore, the presented measurements are all close to the diffusive (dirty metal) regime, and carrier scattering at the sample boundaries alone cannot fully account for the value of the mean free path. The relevance of thermal averaging of phase-coherent effects can be judged from the thermal length $l_{th} = \sqrt{\hbar v_F l/2k_B T} = 700$ nm, which is significantly smaller than L. This indicates that thermal averaging of interference contributions to the conductance is expected to be relevant.

3.2. *Aharonov–Bohm measurements*

Figure 2(a) displays the four-terminal resistance of the ring as a function of magnetic field at $V_{BG} = -5.789$ V. The raw data trace shows a strong modulation of the background resistance on a magnetic field scale of about 100 mT. Clear periodic oscillations can be seen on top of this background. They have a period in magnetic field $\Delta B_{AB} = 17.9$ mT, indicated by the vertical lines. This period corresponds to the h/e-periodic Aharonov–Bohm oscillations of a ring structure of 271 nm radius, in good agreement with the mean radius r_0 of the ring.

Figure 2(b) shows the same data with the background resistance subtracted. The background was determined by performing a running average over one Aharonov–Bohm period ΔB_{AB}. This method was found to lead to no relevant distortion of the oscillations after background subtraction (with some exception in figure 3 around $B = 0$ T, which is of minor importance for this paper). The amplitude of the Aharonov–Bohm oscillations is modulated as

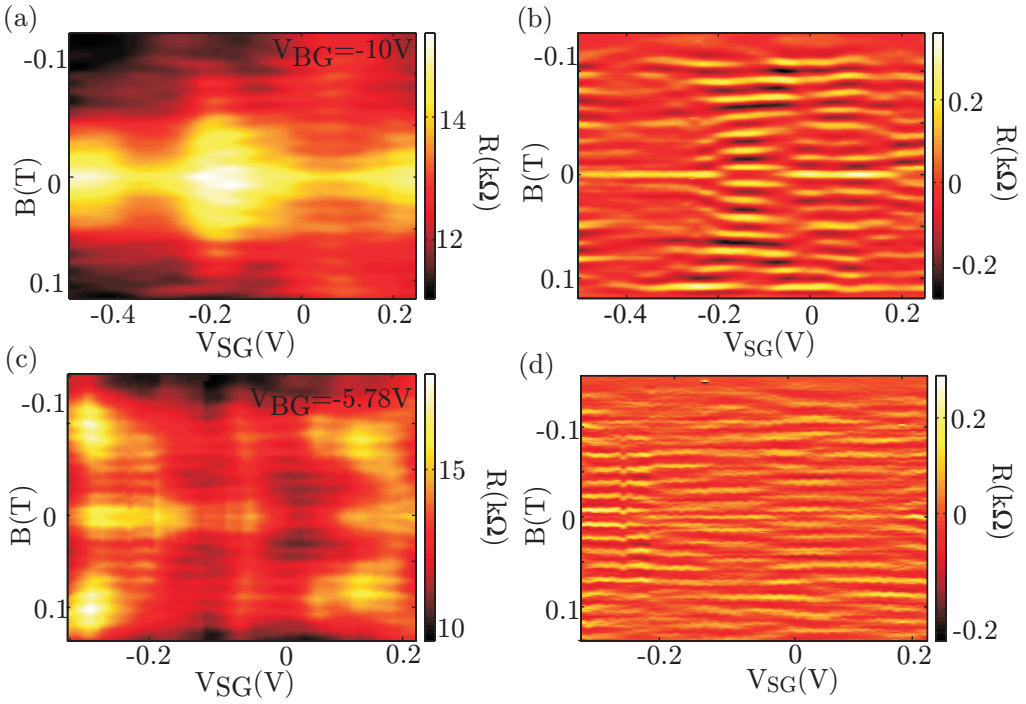

Figure 3. Four-terminal resistance as a function of magnetic field B and voltage applied to SG1 (V_{SG}), measured with a constant current $I = 1$ nA. ((a) and (c)) The raw data, recorded at $V_{BG} = -10$ V and -5.789 V. ((b) and (d)) The corresponding data where the background has been removed for each individual trace by averaging over one Aharonov–Bohm period in the magnetic field.

a function of magnetic field on the same scale as the background resistance, indicating that a finite number of paths enclosing a range of different areas contribute to the oscillations. This observation is compatible with the finite width W of the ring [25].

In figure 2(c), the fast Fourier transform (FFT) of the data in figure 2(a) is plotted. The peak seen at $60\,mT^{-1}$ corresponds to the h/e-periodic Aharonov–Bohm effect. The width of this peak is significantly smaller than the range of frequencies expected from the range of possible enclosed areas in our geometry (indicated as a gray-shaded region in figure 2(c)).

Geometrically, the sample has an aspect ratio of length L to width W of about $L/W = 7.5$ as discussed above. When evaluating the resistance of the sample at the Dirac point (figure 1(c)), we find it to be eighteen times $h/4e^2$, which yields an aspect ratio of $L/W = 18$, given that most graphene samples have a resistivity of $h/4e^2$ at the charge neutrality point. The geometrical aspect ratio is roughly one-third of this aspect ratio estimated from the sample resistance at the charge neutrality point. Similarly, the FFT-peak width of one R(B)-trace is only one-third of the peak width expected from the geometry sample dimensions.

We therefore speculate that the paths contributing to transport, in general, and to the Aharonov–Bohm effect, in particular, may not cover the entire geometric area of the ring arms. One possible interpretation is that the sample has rough unordered edges leading to a region along the edges that does not contribute to the electrical transport.

In this four-contact measurement, the oscillations have a relative amplitude $\Delta R_{AB}/R_{total}$ of more than 5%. Considering that the resistance of the ring is only about 40% of the total measured resistance R_{total}, this corresponds to a relative change of 12% of the ring resistance.

In general, the observed Aharonov–Bohm oscillations become more pronounced for smaller current levels, as expected. The current level of 5 nA was chosen as a good compromise between the signal-to-noise ratio of the voltage measurement and the visibility of the Aharonov–Bohm oscillations. However, due to limited sample stability, the visibility of the oscillations at a given back gate voltage depends on the back gate voltage history. Therefore measurements presented here were taken over only small ranges of back gate voltage after having allowed the sample to stabilize in this range.

Higher harmonics, especially $h/2e$-periodic oscillations, are not visible in the magnetoresistance traces, nor do they lead to a clear peak in the Fourier spectrum ($<1\%$ of the h/e-oscillation amplitude). This indicates that the phase coherence length $l_\varphi < 2L$, i.e. it is (significantly) smaller than twice the circumference of the ring. Given the temperature of our experiment, this estimate is very well compatible with the phase-coherence lengths reported in [13], [26]–[28].

The measurements were taken in a magnetic field range where the classical cyclotron radius $R_c = \hbar k_F/eB > 640\,\text{nm}$ is bigger than the mean free path l, the ring width W and even the ring diameter. At the same time, Landau level quantization effects are negligible, because the sample is studied in the low-field regime $\mu B \ll 1$. The only relevant effect of the magnetic field on the charge carrier dynamics is therefore caused by the field-induced Aharonov–Bohm phase.

In diffusive ring-shaped systems, conductance fluctuations can coexist with Aharonov–Bohm oscillations. However, the relevant magnetic field scale of the conductance fluctuations $\Delta B_{CF} \sim \phi_0/Wl_\varphi$ ($\phi_0 = h/e$) can be forced to be well separated from $\Delta B_{AB} = \phi_0/\pi r_0^2$ by choosing a sufficiently large aspect ratio r_0/W. Judging the situation from the measurement traces in figure 2(a), the only candidates for conductance fluctuations are the magnetic field-dependent variations of the background resistance, which occur on a magnetic field scale that is at least a factor of five larger than ΔB_{AB}. As far as the amplitude of modulation of the background can be estimated from figure 2(a), it is of the order of the conductance quantum e^2/h, which is reasonable, since the condition $l_\varphi \sim L$ implies the absence of strong self-averaging over the ring circumference L.

3.3. *Side-gate-induced phase-shifts*

Figure 3 displays the four-terminal resistance of the ring as a function of magnetic field and voltage V_{SG} applied to the side gate SG1, for two different back gate voltages without (figures 3(a) and (c)) and with (figures 3(b) and (d)) background subtraction.

In the raw data (figures 3(a) and (c)), a modulation of the background resistance on a magnetic field scale, similar to that in figure 2(a), can be observed. The subtraction of the background (extracted as described before) makes the Aharonov–Bohm oscillations visible (figures 3(b) and (d)). Aharonov–Bohm oscillations at different V_{SG} values display either a minimum or a maximum at $B = 0\,\text{T}$, with abrupt changes between the two cases at certain side gate voltage values. This behavior is compatible with the generalized Onsager symmetry requirement for two-terminal resistance measurements, $R(B) = R(-B)$. Although our measurement has been performed in four-terminal configuration, the contact arrangement with respect to the ring and the fact that the contacts are separated by distances $\geqslant l_\phi$ from the

ring lead to a setup where the two-terminal symmetry is still very strong (cf figure 1(a)). Closer inspection shows that the antisymmetric part in the magnetic field of each trace (not shown) is more than a factor of 10 smaller than the symmetric part.

In previous studies on metal rings, the effect of electric fields on the Aharonov–Bohm oscillations has been investigated, and two possible scenarios were discussed: [29] on the one hand, the electric field may shift electron paths in space and thereby change the interference. On the other hand, the electric field may change the electron density and thereby the Fermi wavelength of the carriers. We discuss the latter effect in more detail below, since the relative change in the Fermi wavelength is expected to be more pronounced in graphene compared to conventional metals.

In order to estimate which phase change $\Delta\varphi$ an electronic wave picks up on the scale of the side gate voltage change ΔV_{SG} on which Aharonov–Bohm maxima switch to minima, we use the relation $\Delta\varphi = \Delta k_{\mathrm{F}} L_{\mathrm{eff}}$, where L_{eff}, being the effective length of a characteristic diffusive path, is assumed to be independent of the side gate voltage[4], whereas the change in wave number Δk_{F} is assumed to be caused by ΔV_{SG}. The quantity Δk_{F} is found from the density change Δp_{s} using $\Delta k_{\mathrm{F}} = \sqrt{\pi/4p_{\mathrm{s}}}\Delta p_{\mathrm{s}}$. The density change is related via a parallel plate capacitor model to a change in back gate voltage, i.e. $\Delta p_{\mathrm{s}} = \Delta V_{\mathrm{BG}}\epsilon\epsilon_0/ed$ (where ϵ is the relative dielectric constant of the silicon dioxide substrate and d is the thickness of the oxide layer), leading to $\Delta p_{\mathrm{s}}/\Delta V_{\mathrm{BG}} \approx 7.5 \times 10^{10}\,\mathrm{cm}^{-2}\,\mathrm{V}^{-1}$. Finally, ΔV_{BG} is related to ΔV_{SG} via the lever arm ratio $\alpha_{\mathrm{SG}}/\alpha_{\mathrm{BG}}$.

In order to determine this lever arm ratio, we have performed measurements of conductance fluctuations in the plane of the back gate voltage V_{BG} and the side gate voltage V_{SG} (not shown). The characteristic slope of fluctuation minima and maxima in this parameter plane allows us to estimate the lever arm ratio $\alpha_{\mathrm{SG}}/\alpha_{\mathrm{BG}} \approx 0.2$. In previous experiments on side-gated graphene Hall bars [30], we found a similar lever arm for regions close to the edge of the Hall bar whose width is roughly comparable to the width of the arms of the ring investigated here.

Using the numbers given above and using the density $p_{\mathrm{s}} = 1.2 \times 10^{12}\,\mathrm{cm}^{-2}$ for figure 3(b), we find $\Delta k_{\mathrm{F}} \approx 1.2 \times 10^{6}\,\mathrm{m}^{-1}\mathrm{V}^{-1}\Delta V_{\mathrm{SG}}$. In ballistic systems, the effective length of a path is given by $L_{\mathrm{eff}} \sim L$, giving $\Delta\varphi \approx \Delta V_{\mathrm{SG}}\pi/1.5\,\mathrm{V}$. A phase change of π would imply a change of side gate voltage on the scale of 1.5 V, which is large compared with the measurement in figure 3(b), where this scale is of the order of 100 mV. However, in the diffusive regime, a characteristic path contributing to Aharonov–Bohm oscillations is longer by a factor of $L/l \approx 27$ due to multiple scattering [31] (determined using μ= 5000 $\mathrm{cm}^2/\mathrm{Vs}$), giving $\Delta\varphi \approx \Delta V_{\mathrm{SG}}\pi/55\,\mathrm{mV}$. A change of the side gate voltage of typically 55 mV would cause a switch of the Aharonov–Bohm phase by π, in better agreement with the observation than the ballistic estimate. The same calculation could be used to estimate the correlation voltage of the conductance fluctuations of the background resistance, in agreement with the observation in figures 2 and 3. This correlation voltage is on the same scale as the phase jumps of the Aharonov–Bohm oscillations.

[4] We remark here that this assumption, and the reasoning based on it as given in the main text, corresponds to the usual argument made for dirty metals. However, in graphene, the typical length $L_{\mathrm{eff}} = L^2/l$ of a diffusive path [31] is proportional to k_{F}^{-1}, such that the phase $k_{\mathrm{F}}L_{\mathrm{eff}}$ accumulated along such a path is independent of k_{F} and therefore independent of carrier density and gate voltage. It therefore remains unclear to us how the concept of the Thouless energy as an energy scale for wave function correlations can be transferred to the graphene system. We nevertheless discuss the estimate based on the assumption of a k_{F}-independent L_{eff} (1) in the absence of any better theory and (2) in accordance with [13].

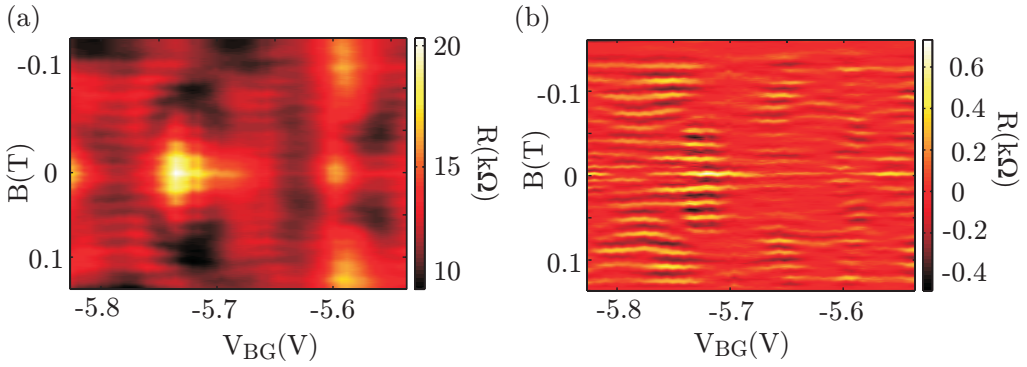

Figure 4. Four-terminal resistance as a function of magnetic field and back gate voltage measured with a constant current of 1 nA. In (a), the raw data are shown, while for (b), the background has been removed.

3.4. Back-gate-induced phase shifts

Figure 4 shows magnetoresistance data for varying back gate voltages and $V_{SG} = 0\,V$. Similar to the case where the side gate was tuned, we observe variations of the oscillation patterns as well as π-phase shifts. The raw data displayed in figure 4(a) show background fluctuations with h/e-periodic Aharonov–Bohm oscillations superimposed. In figure 4(b), the background has been removed. Again, alternating minima and maxima at $B = 0\,T$ can be observed.

The larger visibility of Aharonov–Bohm oscillations observed in our sample, compared with the work in [13], is unlikely to be caused by better material or sample quality. Also, our measurement temperature is about a factor of 4 higher than the lowest temperatures reported there. We therefore believe that the smaller ring dimensions in combination with the four-terminal arrangement may be responsible for the larger value of the visibility observed in our experiment. In [13], the expression [25] $\Delta G \propto l_{th}/l_\varphi \exp(-\pi r_0/l_\varphi)$ was invoked to explain the observed $T^{-1/2}$-dependence of the oscillation amplitude. The exponential term on the right-hand side contains the radius of the ring r_0. A smaller radius will lead to a larger oscillation amplitude, which may explain the improved amplitude in our measurements. However, trying to relate the visibilities observed in the two experiments quantitatively (assuming that all experimental parameters except the ring radius are the same) would lead to a phase-coherence length l_φ smaller than the ring circumference L and only slightly larger than the ring radius r_0. As our experiment demonstrates, a separation of h/e-periodic oscillations from background variations due to magnetoconductance fluctuations is still possible in our device despite the aspect ratio r_0/W, which is reduced in our device compared to [13]. A phase-coherence length between L and r_0 is also compatible with the observation $\Delta B_{CF}/\Delta B_{AB} \approx 5$.

We also note that the diffusive regime investigated in our device is quite extended in back gate voltage. Assuming diffusive scattering at the edges to become dominant as soon as $l \approx W$, we estimate that this does not occur (for transport in the valence band) until V_{BG} becomes more negative than $-80\,V$. Transport may also enter a different regime, when the Fermi wavelength becomes larger than l, which is expected to happen (again for transport in the valence band and assuming $\mu = 5000\,cm^2/Vs$) at back gate voltages larger than $+2\,V$ in our sample. An even different regime may be entered at a back gate voltage of $+9.3\,V$, where $\lambda_F \approx W$. As a consequence, the 'dirty metal' description of the Aharonov–Bohm oscillations should be

applicable in the whole range of back gate voltages shown in figure 1(c), except for a region of ± 8 V around the charge neutrality point, where the resistance is maximum.

4. Conclusion

Even though graphene rings have been analyzed in detail theoretically, there has been only one experimental study until now [13]. In this work, we have studied the Aharonov–Bohm effect in graphene in a two-terminal ring, but using a four-contact geometry. This increases the relative contribution of the ring resistance to the total measured resistance, and together with the smaller ring radius, it allows us to achieve a higher visibility of the oscillations of about 5%. The data are analyzed by a simple dirty metal model justified by a comparison of the different length scales characterizing the system.

The main advantage of graphene compared to metals for Aharonov–Bohm studies is the reduced screening. This makes it possible to use external gates for locally tuning the density and the Fermi wave vector in one of the arms and therefore allows us to observe the electrostatic Aharonov–Bohm effect without the use of tunnel barriers in the arms of the ring. We have shown that by changing the voltage applied to one of the side gates, we can induce a phase jump in the oscillations by changing the phase accumulated along this path.

We have observed Aharonov–Bohm oscillations in four-terminal measurements on a side-gated graphene ring structure. The visibility of the oscillations is found to be about 5%. By changing the voltage applied to the lateral side gate, or the back gate, we observe phase jumps of π compatible with the generalized Onsager relations for two-terminal measurements. The observations are in good agreement with an interpretation in terms of diffusive metallic transport in a ring geometry.

Acknowledgments

We acknowledge the support of the ETH FIRST laboratory and the financial support of EH Zuerich and the Swiss Science Foundation (Schweizerischer Nationalfonds, NCCR Nanoscience).

References

[1] Novoselov K S, Geim A K, Morozov S V, Jiang D, Zhang Y, Dubonos S V, Grigorieva I V and Firsov A A 2004 *Science* **306** 666
[2] Han M Y, Ozyilmaz B, Zhang Y and Kim P 2007 *Phys. Rev. Lett.* **98** 206805
[3] Chen Z, Lin Y-M, Rooks M J and Avouris P 2007 *Physica* E **40/2** 228
[4] Liu X, Oostinga J B, Morpurgo A F and Vandersypen L M K 2009 *Phys. Rev.* B **80** 121407
[5] Todd K, Chou H, Amasha S and Goldhaber-Gordon D 2009 *Nano Lett.* **9** 1
[6] Molitor F, Jacobsen A, Stampfer C, Güttinger J, Ihn T and Ensslin K 2009 *Phys. Rev.* B **79** 075426
[7] Stampfer C, Güttinger J, Hellmüller S, Molitor F, Ensslin K and Ihn T 2009 *Phys. Rev. Lett.* **102** 056403
[8] Ponomarenko L A, Schedin F, Katsnelson M I, Yang R, Hill E H, Novoselov K S and Geim A K 2008 *Science* **320** 356
[9] Stampfer C, Güttinger J, Molitor F, Graf D, Ihn T and Ensslin K 2008 *Appl. Phys. Lett.* **92** 012102
[10] Stampfer C, Schurtenberger E, Molitor F, Güttinger J, Ihn T and Ensslin K 2008 *Nano Lett.* **8** 2378

[11] Schnez S, Molitor F, Stampfer C, Güttinger J, Shorubalko I, Ihn T and Ensslin K 2009 *Appl. Phys. Lett.* **94** 012107
[12] Molitor F, Drscher S, Güttinger J, Jacobsen A, Stampfer C, Ihn T and Ensslin K 2009 *Appl. Phys. Lett.* **94** 222107
[13] Russo S, Oostinga J B, Wehenkel D, Heersche H B, Shams Sobhani S, Vandersypen L M K and Mopurgo A F 2008 *Phys. Rev.* B **77** 085413
[14] Aharonov Y and Bohm D 1959 *Phys. Rev.* **115** 485
[15] Webb R A, Washburn S, Umbach C P and Laibowith R B 1985 *Phys. Rev. Lett.* **54** 2696
[16] Recher P, Trauzettel B, Rycerz A, Blanter Y M, Beenakker C W J and Morpurgo A F 2007 *Phys. Rev.* B **76** 235404
[17] Rycerz A 2009 *Act. Phys. Pol.* A **115** 322
[18] Tikhonenko F V, Horsell D W, Gorbachev R V and Savchenko A K 2008 *Phys. Rev. Lett.* **100** 056802
[19] Gorbachev R V, Tikhonenko F V, Mayorov A S, Horsell D W and Savchenko A K 2007 *Phys. Rev. Lett.* **98** 176805
[20] Tikhonenko F V, Kozikov A A, Savchenko A K and Gorbachev R V 2009 *Phys. Rev. Lett.* **103** 226801
[21] Bachtold A *et al* 1999 *Nature* **397** 673
[22] Cao J *et al* 2004 *Phys. Rev. Lett.* **93** 216803
[23] Ferrari A C *et al* 2006 *Phys. Rev. Lett.* **97** 187401
[24] Graf D, Molitor F, Ensslin K, Stampfer C, Jungen A, Hierold C and Wirtz L 2007 *Nano Lett.* **7** 238
[25] Washburn S and Webb R A 1986 *Adv. Phys.* **35** 375
[26] Graf D, Molitor F, Ihn T and Ensslin K 2007 *Phys. Rev.* B **75** 245429
[27] Miao F, Wijeratne S, Zhang Y, Coskun U C, Bao W and Lau C N 2007 *Science* **317** 1530
[28] Berger C *et al* 2006 *Science* **312** 1191
[29] Washburn S, Schmid H, Kern D and Webb R A 1987 *Phys. Rev. Lett.* **59** 1791
de Vegvar P G N, Timp G, Mankiewich P M, Behringer R and Cunningham J 1989 *Phys. Rev.* B **40** 3491
[30] Molitor F, Güttinger J, Stampfer C, Graf D, Ihn T and Ensslin K 2007 *Phys. Rev.* B **76** 245426
[31] Imry Y 2002 *Introduction to Mesoscopic Physics* 2nd edn (New York: Oxford University Press) p 73